LQR CONTROL ON LINEAR MODEL OF FLEXIBLE INVERTED PENDULUM

Tran Ngoc Son, Nguyen Minh Tam, Nguyen Van Dong Hai
Ho Chi Minh City University of Technology and Education (HCMUTE), Vietnam

Received 30/7/2018, Peer reviewed 03/01/2019, Accepted for publication 22/03/2019

ABSTRACT

Most kinds of robots in researches are in solid structures. In these models, Euler-Lagrange method is easily used to obtain dynamic equations for simulation and obtaining controllers. But, actually, there is always flexibility - even very small or remarkable – in all kinds of robots. This research solves a problem in modelling a complex robot with a flexible link-flexible inverted pendulum- by presenting a method to simplify that robot. Thence, controller and simulation of controlling model can be tested. The flexible inverted pendulum is a distributed parameter system which is developed from cart and pole system, a robot with all solid links. An investigation of applying LQR control on this model is examined. In simulation, approximated dynamic equations are presented. The knowledge of the structure of the model leads to designing a linear LQR controller. Genetic algorithm is successfully utilized to optimize the controller. After a survey in a simulation, a hardware platform is presented and tested. In an experiment, LQR is proven to work well and suit theoretical points.

Keywords: *Flexible inverted pendulum; Inverted pendulum on Cart; Distributed parameter system; LQR control; Genetic algorithm.*

1. INTRODUCTION

Inverted pendulum (IP) is a classical model in control laboratories. Most researches on these models are based on solid links, such as rotary IP, cart and pole system, pendubot [1]… To widen the research to robots with elastic links through IP, researches are shown in [2]-[4]. In those studies, solid pendulums are replaced by an elastic beam, called flexible IP (FIP). It is proven that a free-moving pendulum on cart causes un-stability of FIP [5]. Thence, a model of fixing IP on a cart is presented in [6]. Also in that research, distributed parameter model (DPM) of FIP is simplified to linear form as in Fig. 1. Solving a DPM control problem is complicated and it is still an open direction until now [7]. This classical research [6] gives a simple direction to simplify a PDM problem into a model that is equivalent to a non-PDM. Then, tools that are used for non-PDM can be applied. A PD controller was introduced in that study [6]. Anyway, PD controller is not based on mathematical background. LQR control [8], which has the same simple structure as PD and well-balanced control many SIMO (single-input multi-output) systems, is a solution. Actually, according to control quality, LQR is not better than other controllers, such as, PID and nonlinear controller. The controllers will give better responses if better control parameters are chosen (in LQR control, they are matrixes Q, R; in PID control, they are K_p, K_i, K_d; in sliding mode control, they are sliding surfaces and sliding parameters…). Therefore, in this paper, the comparison among kinds of controllers is not focused. But, we focus on creating a FIP platform in both hardware and software for survey in LQR controller. The success in making this platform can be based for other control algorithms on this DPM. In a simulation, genetic algorithm (GA) is utilized to optimize the control parameters of LQR controller for better control quality. Besides, in real model, only control parameters of LQR are examined without the optimizing by

GA. The changing these control parameters shows that controller suits the theory of optimal control. Anyway, not using GA in real model is a deficiency of this paper and authors prefer to solve this problem in next study. By the way, control FIP by LQR in this paper is the pioneer contribution that has not been operated before.

This paper concludes 6 sections. Section 1 introduces the paper. Section 2 presents the dynamic equations of FIP. In Section 3, a process of LQR controller is shown. In the simulation of section 4, LQR is proved to work well and this controller is optimized by GA successfully. In Section 5, a hardware platform of FIP is shown and a survey of FIP by this platform shows that real-time LQR controller not only works well but also suits the theoretical points. In Section 6, a conclusion ends the paper.

2. DYNAMIC EQUATIONS

From [5], FIP is a DPM. Controllers for these kinds of models are still researched and no effective controllers are presented for FIP. Thence, in [6], a linear form for FIP is presented as in Fig. 1. In this research, equations and inequalities (1)-(18) are obtained. Two variables α_1 and α_2 show the condition of the flexible beam. Motions of two points, which are at the top and in the middle of the beam, are the same as under the effects of two virtual springs (as in Fig. 1). With this approximation, the model in Fig. 1 is simplified as:

$$X_1 \approx l_2 \sin\alpha_1;\ Y_1 \approx l_2 \cos\alpha_1 \tag{1}$$

$$X_2 \approx l_1 \sin\alpha_2;\ Y_2 \approx l_1 \cos\alpha_2 \tag{2}$$

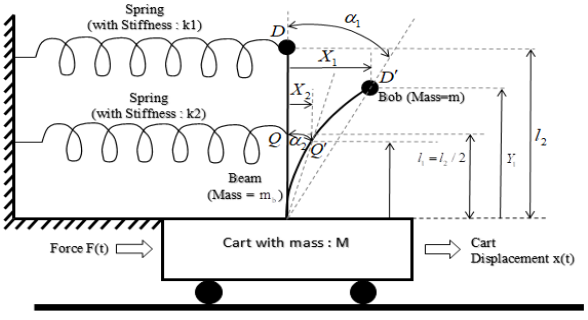

***Fig. 1** FIP linear model*

The potential energy is

$$P = \frac{k_1\left(l_2\sin\alpha_1\right)^2}{2} - mgl_2\left(1-\cos\alpha_1\right) + \\ + \frac{k_2\left(l_1\sin\alpha_2\right)^2}{2} - m_b g l_1\left(1-\cos\alpha_2\right) \tag{3}$$

The kinetic energy is

$$K = \frac{M}{2}\left(\dot{x}\right)^2 + \frac{m_b}{2}\left[\left(\dot{x}+\dot{X}_2\right)^2 + \left(\dot{Y}_2\right)^2\right] + \\ + \frac{m}{2}\left[\left(\dot{x}+\dot{X}_1+\dot{X}_2\right)^2 + \left(\dot{Y}_1+\dot{Y}_2\right)^2\right] \tag{4}$$

The Lagrangian operator can be developed as

$$L = \frac{M\dot{x}^2}{2} + \frac{m_b}{2}\begin{bmatrix}\dot{x}^2 + 2l_1\dot{x}\dot{\alpha}_2\cos\alpha_2 + \\ + l_1{}^2\dot{\alpha}_2{}^2\end{bmatrix} + \\ + \frac{m}{2}\begin{bmatrix}\dot{x}^2 + 2\dot{x}\begin{pmatrix}l_2\dot{\alpha}_1\cos\alpha_1 + \\ + l_1\dot{\alpha}_2\cos\alpha_2\end{pmatrix} + l_2{}^2\dot{\alpha}_1{}^2 + \\ + l_1{}^2\dot{\alpha}_2{}^2 + 2l_2l_1\dot{\alpha}_1\dot{\alpha}_2\cos\left(\alpha_1-\alpha_2\right)\end{bmatrix} + \\ + mgl_2\left(1-\cos\alpha_1\right) - \frac{k_1}{2}\left(l_2\sin\alpha_1\right)^2 + \\ + m_b g l_1\left(1-\cos\alpha_2\right) - \frac{k_2}{2}\left(l_1\sin\alpha_2\right)^2 \tag{5}$$

Consider the Rayleigh dampling coefficient as in (6)

$$R_d = \frac{b_3}{2}(\dot{x})^2 + \frac{b_2}{2}[(\dot{x}+\dot{X}_2)^2 + (\dot{Y}_2)^2] + \\ + \frac{b_1}{2}[(\dot{x}+\dot{X}_1+\dot{X}_2)^2 + (\dot{Y}_1+\dot{Y}_2)^2] \tag{6}$$

Euler-Lagrange dynamic equations are

$$\frac{d}{dt}\left(\frac{\partial L}{\partial\dot{\alpha}_1}\right) - \frac{\partial L}{\partial\alpha_1} = 0 \tag{7}$$

$$\frac{d}{dt}\left(\frac{\partial L}{\partial\dot{x}}\right) - \frac{\partial L}{\partial x} = F \tag{8}$$

$$\frac{d}{dt}\left(\frac{\partial L}{\partial\dot{\alpha}_2}\right) - \frac{\partial L}{\partial\alpha_2} = 0 \tag{9}$$

After calculations, (7)-(9) become

$$ml_2^2\ddot{\alpha}_1 + ml_2\ddot{x}\cos\alpha_1 + ml_2l_1\ddot{\alpha}_2\cos(\alpha_1-\alpha_2) + \frac{k_1l_2^2\sin 2\alpha_1}{2} + b_1l_2^2\dot{\alpha}_1 - mgl_2\sin\alpha_1 + b_1l_2\dot{x}\cos\alpha_1 + \quad (10)$$
$$+b_1l_2l_1\dot{\alpha}_2\cos(\alpha_1-\alpha_2) + ml_2l_1\dot{\alpha}_2^2\sin(\alpha_1-\alpha_2) = 0$$

$$(m+m_b)l_1^2\ddot{\alpha}_2 + (m+m_b)l_1\ddot{x}\cos\alpha_2 + ml_2l_1\ddot{\alpha}_1\cos(\alpha_1-\alpha_2) + (b_1+b_2)l_1\dot{x}\cos\alpha_2 + (b_1+b_2)l_1^2\dot{\alpha}_2 + \quad (11)$$
$$+b_1l_2l_1\dot{\alpha}_1\cos(\alpha_1-\alpha_2) - ml_2l_1\dot{\alpha}_1^2\sin(\alpha_1-\alpha_2) + \left(k_2l_1^2\sin 2\alpha_2\right)/2 - m_bgl_1\sin\alpha_2 = 0$$

$$\left(M+m_b+m\right)\ddot{x} + (m+m_b)l_1\left(\ddot{\alpha}_2\cos\alpha_2 - \dot{\alpha}_2^2\sin\alpha_2\right) + ml_2\left(\ddot{\alpha}_1\cos\alpha_1 - \dot{\alpha}_1^2\sin\alpha_1\right) + \left(b_1+b_2+b_3\right)\dot{x} + \quad (12)$$
$$+(b_1+b_2)l_1\dot{\alpha}_2\cos\alpha_2 + b_1l_2\dot{\alpha}_1\cos\alpha_1 = F$$

System parameters and variables in (10)-(12) are listed in Table 1 below

Table 1. *System parameters and variables of FIP*

Para-meters/ Variables	Description	Unit
M	Mass of cart	kg
m_b	Mass of beam	kg
M	Mass of bob	kg
l_1	Half of length of beam	m
l_2	Length of beam	M
k_1	Spring stiffness of bob	*N/m*
k_2	Spring stiffness of beam	*N/m*
b_1	Damping coefficient of bob	kgm^2
b_2	Damping coefficient of beam	kgm^2
b_3	Damping coefficient of cart	kgm^2
G	Gravitation acceleration	m/s^2
X	Position of cart	*M*
α_1	Angle of middle point of beam and vertical axis	rad
α_2	Angle of tip mass and vertical axis	rad

Dynamic equations in (10)-(12) can be transformed to matrix form as

$$\dot{\sigma} = \mathbb{Q}_1(\sigma) + \mathbb{Q}_2(\sigma)F \quad (13)$$

where: $\sigma = \left[\alpha_1 \quad \dot{\alpha}_1 \quad x \quad \dot{x} \quad \alpha_2 \quad \dot{\alpha}_2\right]^T$

Critical buckling load for fixed-free beam is

$$T_C = \left(\pi^2 EI\right)/4l_2^2 \quad (14)$$

Load of the tip is

$$T_L = mg \quad (15)$$

In order to be able to control the FIP on upside position, we have to select system parameters to satisfy this inequality

$$T_L < T_C \quad (16)$$

3. CONTROL ALGORITHM

If (16) is satisfied, the equilibrium solution (all velocity and position components are zero) is imposed as

$$(1/2)k_1l_2^2\sin(2\alpha_1) - mgl_2\sin\alpha_1 = 0 \quad (17)$$

$$(1/2)k_2l_1^2\sin(2\alpha_2) - m_bgl_1\sin\alpha_2 = 0 \quad (18)$$

A solution of (17) and (18) is obviously $[\alpha_1, \alpha_2] = [0, 0]$.

In order to make a simulation of LQR controller closed to real-time model, dynamic equations of motor have to be concerned and implemented into a system. In [9], the nonlinear model of DC motor is presented through Fig. 2 and (19).

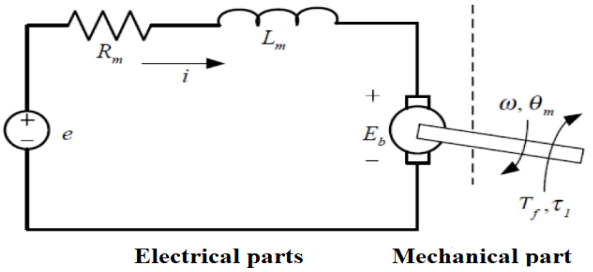

Fig. 2. *The model of DC servo motor*

Relation of voltage on motor and force which is created by operation of motor is

$$F = \frac{d_l}{R_c}\left[\frac{K_t}{R_m}e - d_l\left(\frac{K_bK_t}{R_mR_c} + \frac{C_m}{R_c}\right)\dot{x} - \frac{J_md_l}{R_c}\ddot{x}\right] \quad (19)$$

Where: $k_1 = \frac{d_1 K_t}{R_m R_c}; k_2 = \frac{d_1^2 K_t K_b}{R_m^2 R_c} + \frac{d_1^2 C_m}{R_c^2}; k_3 = \frac{d_1^2 J_m}{R_m^2}$

Table 2. *System parameters and variables of DC motor*

Parameters/ Variables	Description	Unit
R_c	Wheel radius	m
K_b	Electrical constant	V/rad/s
K_t	Torque constant	Nm/A
C_m	Viscous Friction	Nmsec/rad
F	Force	N
J_m	Moment of inertia	$kg.m^2$
d_1	Gear ratio	No unit
E	Power supply	V
X	Position of cart	m
R_m	Electrical resistance	Ω

Thence, from (13) and (19), after some calculations, dynamic equations with input signal as voltage on DC motor of FIP are generalized as follow form

$$\dot{\sigma} = \Phi_1(\sigma) + \Phi_2(\sigma)e \tag{20}$$

Nonlinear dynamic equations (20) lead to linear form at working point $\sigma = [\alpha_1 \ \dot{\alpha}_1 \ x \ \dot{x} \ \alpha_2 \ \dot{\alpha}_2]^T = [0 \ 0 \ \cdots \ 0]^T$. System matrixes are $\Phi_1 = [\Phi_{11} \ \Phi_{12} \ \Phi_{13} \ \Phi_{14} \ \Phi_{15} \ \Phi_{16}]^T$; $\Phi_2 = [\Phi_{21} \ \Phi_{22} \ \Phi_{23} \ \Phi_{24} \ \Phi_{25} \ \Phi_{26}]^T$. Linearized model of FIP is obtained as

$$\dot{\sigma} = A\sigma + Be \tag{21}$$

Where:

$$A = \begin{bmatrix} \frac{\partial \Phi_{11}}{\partial \sigma_1}\Big|_{\substack{\sigma=\sigma_0 \\ e=0}} & \frac{\partial \Phi_{11}}{\partial \sigma_2}\Big|_{\substack{\sigma=\sigma_0 \\ e=0}} & \cdots & \frac{\partial \Phi_{11}}{\partial \sigma_6}\Big|_{\substack{\sigma=\sigma_0 \\ e=0}} \\ \frac{\partial \Phi_{12}}{\partial \sigma_1}\Big|_{\substack{\sigma=\sigma_0 \\ e=0}} & \frac{\partial \Phi_{12}}{\partial \sigma_2}\Big|_{\substack{\sigma=\sigma_0 \\ e=0}} & \cdots & \frac{\partial \Phi_{12}}{\partial \sigma_6}\Big|_{\substack{\sigma=\sigma_0 \\ e=0}} \\ \vdots & \vdots & \ddots & \vdots \\ \frac{\partial \Phi_{16}}{\partial \sigma_1}\Big|_{\substack{\sigma=\sigma_0 \\ e=0}} & \frac{\partial \Phi_{16}}{\partial \sigma_2}\Big|_{\substack{\sigma=\sigma_0 \\ e=0}} & \cdots & \frac{\partial \Phi_{16}}{\partial \sigma_6}\Big|_{\substack{\sigma=\sigma_0 \\ e=0}} \end{bmatrix} \tag{22}$$

$$B = \begin{bmatrix} \frac{\partial \Phi_{21}}{\partial \sigma_1}\Big|_{\substack{\sigma=\sigma_0 \\ e=0}} & \frac{\partial \Phi_{21}}{\partial \sigma_2}\Big|_{\substack{\sigma=\sigma_0 \\ e=0}} & \cdots & \frac{\partial \Phi_{21}}{\partial \sigma_6}\Big|_{\substack{\sigma=\sigma_0 \\ e=0}} \\ \frac{\partial \Phi_{22}}{\partial \sigma_1}\Big|_{\substack{\sigma=\sigma_0 \\ e=0}} & \frac{\partial \Phi_{22}}{\partial \sigma_2}\Big|_{\substack{\sigma=\sigma_0 \\ e=0}} & \cdots & \frac{\partial \Phi_{22}}{\partial \sigma_6}\Big|_{\substack{\sigma=\sigma_0 \\ e=0}} \\ \vdots & \vdots & \ddots & \vdots \\ \frac{\partial \Phi_{26}}{\partial \sigma_1}\Big|_{\substack{\sigma=\sigma_0 \\ e=0}} & \frac{\partial \Phi_{26}}{\partial \sigma_2}\Big|_{\substack{\sigma=\sigma_0 \\ e=0}} & \cdots & \frac{\partial \Phi_{26}}{\partial \sigma_6}\Big|_{\substack{\sigma=\sigma_0 \\ e=0}} \end{bmatrix} \tag{23}$$

and equilibrium point $\sigma_0 = [0 \ \ 0 \ \ \cdots \ \ 0]^T$

Therefore, with dynamic equations and equilibrium points that are obtained, a simple LQR controller is used. The stability of the system is guaranteed by solving Ricatti equations. Structure of LQR for FIP is shown in Fig. 3. In this figure, linear feedback K is calculated from matrix A, B (in (20)) and selected weighing matrix Q, R. Matlab gives a command to obtain quickly this control matrix as

$$K = lqr(A, B, Q, R) \tag{24}$$

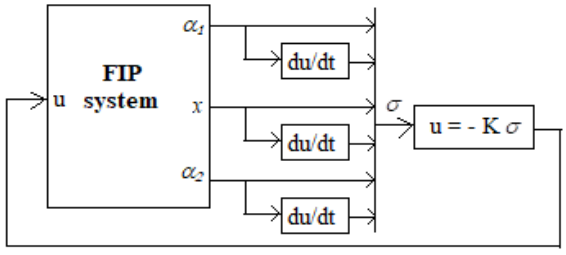

Fig. 3 *LQR control structure for FIP system*

4. SIMULATION

Weighing positive matrixes Q, R can be chosen by trial and error test. Anyway, GA is used to optimize the controller. Simulating system under LQR controller in 10s with sample time as 10ms. There are 1001 samples of system response in a period of simulation time. We choose the fitness function as

$$J = \sum_{i=1}^{1001} \left(e_{1i}^2 + e_{2i}^2 + e_{3i}^2 \right) \tag{25}$$

where e_{1i}, e_{2i}, e_{3i} are the errors between the responses α_1, x, α_2 in simulation and the reference signals of system in Fig. 1 when cart and pendulum are stable in upward position.

Three cases are listed as below and simulation results are shown in *Fig. 4*. In (26)-(28), after generations, function J decreases (Fig. 5). Correspondingly, with smaller J, the setting time and overshoot of each case decrease and it yields better quality control (from Fig. 4). Thence, from simulation, LQR controller is proved to work well and GA actually optimizes LQR controller.

Case 1: At generation 1

$$Q=\begin{bmatrix}508.1&0&0&0&0&0\\0&0.8&0&0&0&0\\0&0&341.7&0&0&0\\0&0&0&7.31&0&0\\0&0&0&0&283.7&0\\0&0&0&0&0&0.19\end{bmatrix};\quad R=1; \tag{26}$$

$$K=\begin{bmatrix}-17.4875&0.1407&50.1482&-6.6434&-32.6294&-2.7096\end{bmatrix};$$

$$J=J_1=16.9364$$

Case 2: At generation 10

$$Q=\begin{bmatrix}29.8&0&0&0&0&0\\0&0.45&0&0&0&0\\0&0&341.5&0&0&0\\0&0&0&11.77&0&0\\0&0&0&0&950.7&0\\0&0&0&0&0&1.19\end{bmatrix};\quad R=1; \tag{27}$$

$$K=\begin{bmatrix}-12.0827&-0.2162&32.2998&-4.6757&-45.0554&-2.8402\end{bmatrix};$$

$$J=J_2=10.5097$$

Case 3: At generation 23

$$Q=\begin{bmatrix}23.1&0&0&0&0&0\\0&1.66&0&0&0&0\\0&0&10.2&0&0&0\\0&0&0&2.27&0&0\\0&0&0&0&924&0\\0&0&0&0&0&1\end{bmatrix};\quad R=1; \tag{28}$$

$$K=\begin{bmatrix}-14.2148&0.4197&30.1171&-3.0343&-44.6581&-2.4607\end{bmatrix};$$

$$J=J_3=8.5690$$

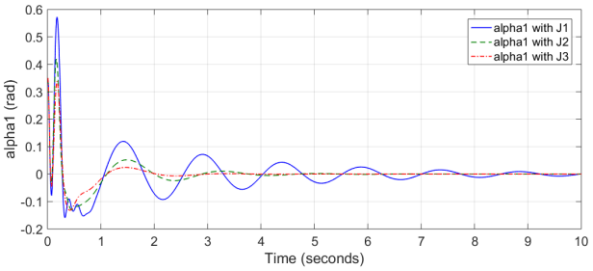

(a)

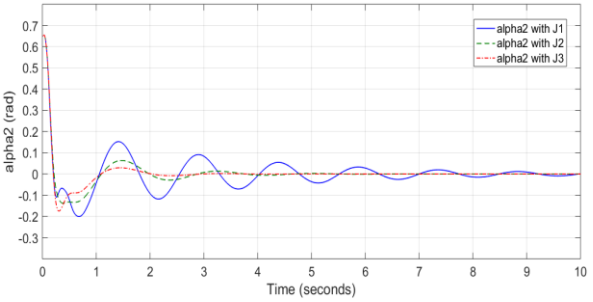

(b)

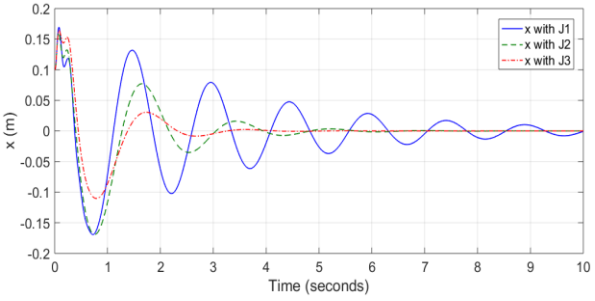

(c)

Fig. 4 *Comparison of FIP responses by GA*

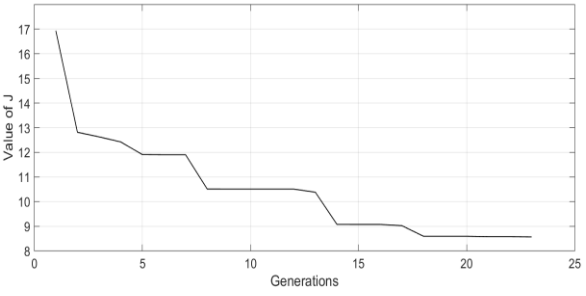

Fig. 5 *Values of fitness function J through generations*

5. EXPERIMENT

5.1. Hardware platform

An experimental FIP platform is presented in *Fig. 6* below. MPU sensor is located at the middle of the elastic beam to measure an angle α_2. Another MPU sensor

is located at the top of the elastic beam to measure an angle α_1. The tip mass should be sufficiently small to satisfy the formula (16). Arduino MEGA is used to implement the control. The elastic beam is made of suitable plastic to let the first- order mode shape of vibration be concerned.

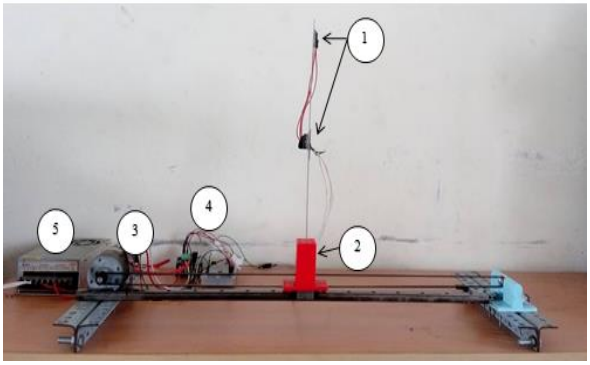

(a)

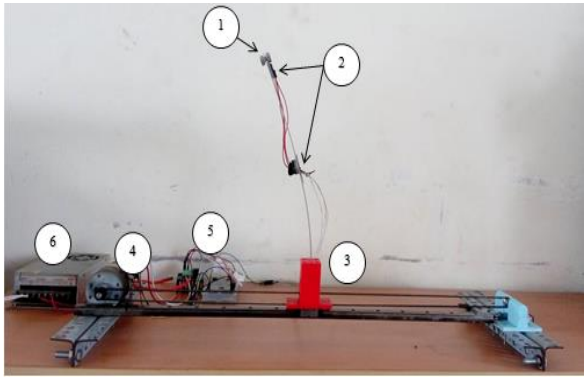

(b)

Fig. 6 *Experimental model of FIP*

1- Bob
2- Sensor MPUs 6050
3- Cart
4- 24VDC Motor
5- Arduino Mega2560 and H-Bridge
6- DC Source

Values of system parameters in Table 1 in the real model are

$$M=0.085(kg);\ m_b=0.015(kg);\ m=0.007(kg);$$
$$l_1=0.14(m)\ ;\quad l_2=0.28(m)\ ;\quad b_1=b_2=0.008\ ; \qquad (29)$$
$$g=9.81(m/s^2);\ k_1=2.1(N/m);\ k_2=8.4(N/m)$$

and values of system parameters in *Table 2* in real model are

$$R_m=6(\Omega)\ ;\quad K_b=0.065(V/(rad/s))\ ;$$
$$K_v=0.065(Nm/A)\ ;\quad J_m=10^{-5}(kgm^2)\ ;$$
$$C_m=6.10^{-5}(Nmsec/rad);\ L_m=0.01(Nmsec/rad) \qquad (30)$$

By observing the responses from figures, the comparison can be concluded. But, a criterion is presented from the idea of fitness function of GA. An evaluating function is presented as

$$J_K=\lambda_1\sum_{i=1}^{\psi}e_{\alpha_1 n}^2+\lambda_2\sum_{i=1}^{\psi}e_{xn}^2+\lambda_3\sum_{i=1}^{\psi}e_{\alpha_2 n}^2 \qquad (31)$$

In this formula, $e_{\alpha_1 n}$, $e_{\alpha_2 n}$ and e_{xn} are the errors between angle α_1, α_2, x and their reference signals in sample nth, correspondingly. ψ is the quantity of samples that are collected through simulation. Parameters λ_1, λ_2 and λ_3 are correspondingly weighing parameters that decide the effectiveness of each error to evaluating function J_K. In this study, we select

$$\lambda_1=\lambda_2=\lambda_3=1 \qquad (32)$$

5.2. Experimental results

Because the FIP is a vibrating system, it is better to terminate the velocity of the beam instead of the angle of the beam. By that opinion, terminating velocity of the beam is more concerned than the angle of beam. In an experiment, both q_1, q_2 affect α_1, α_2 in the same way. Parameter q_2 is the velocity of changing of α_1; parameter q_6 presents the velocity of changing of α_6. We assumed that only the first mode shape exists. Thence, only α_1 are examined in experiment. In theory, if values of q_2 are increased, the position of beam tends to be better in quality than other variables, such as shorter settling time, smaller settling error, smaller overshoot. In Fig. 7, when increasing q_2, the vibration of α_1 decreases faster (from Fig. 7 (a1) to (a4)) as in theory. Correspondingly, the position of cart is difficult to be controlled (overshoot

increases from Fig. 7 (b1) to Fig. 7(b4)). Thence, the experiment suits the theoretical point that changing suitable components in weighing matrix Q can control better one variable and may cause worse control quality of other variables.

6. CONCLUSION

In this paper, authors apply LQR controller for a FIP system. A linear approximated model is examined and tested in simulation. The LQR controller is proved to work well. GA is proved to have efficient role in optimizing this controller in simulation. In experiment, a real model is presented. The LQR controller can both control cart position and terminate the vibration of the elastic beam. The control quality can be adjusted by following the LQR control theory.

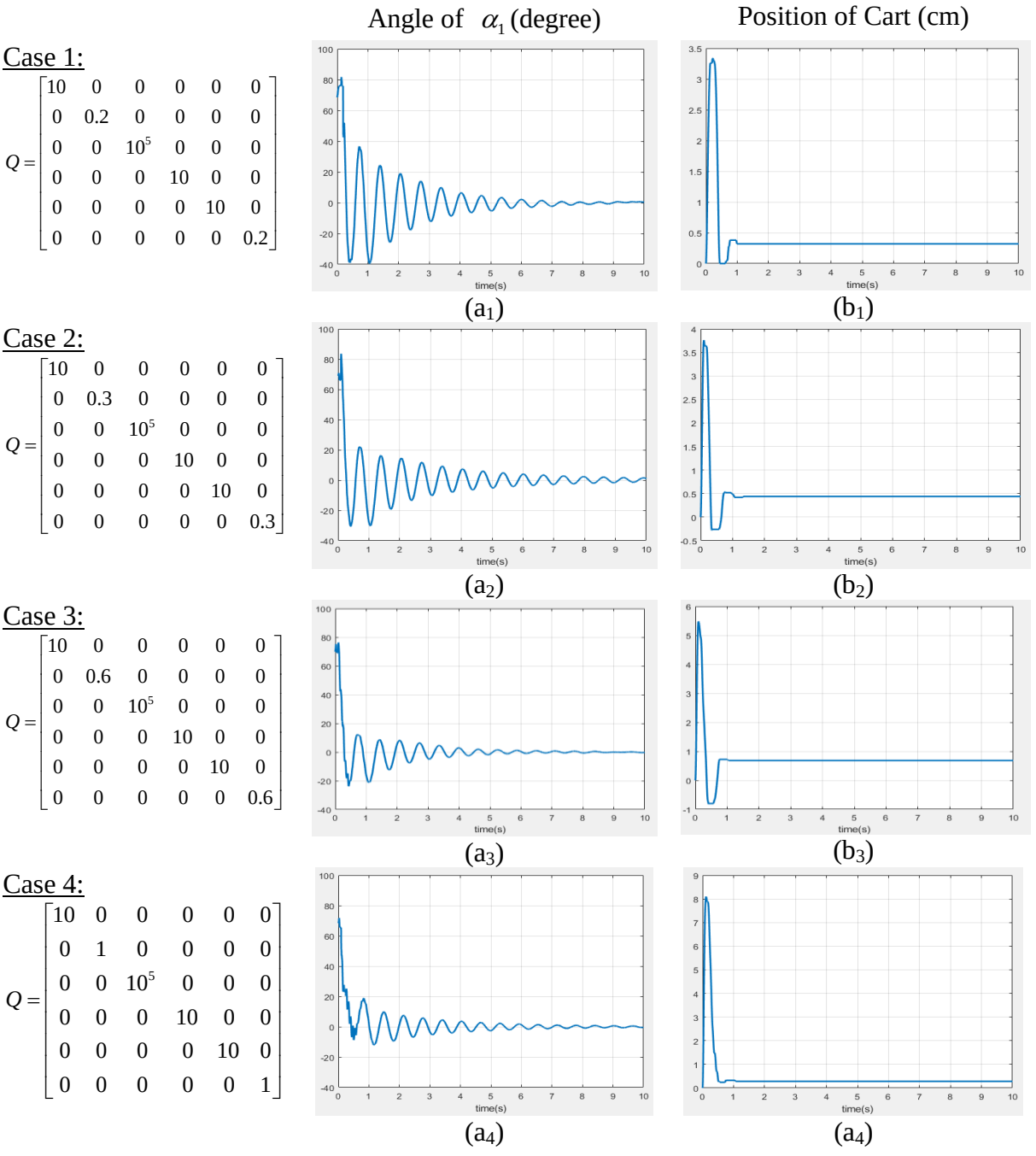

***Fig. 7** Experimental results of FIP*

REFERENCE

[1] Slavka Jadlovska, Jan Sarnovsky, Jaroslav Vojtek, Dominik Voscek, *Advanced Generalized Modeling of Classical Inverted Pendulum Systems*, Emergent Trends in Robotics and Intelligent Systems, pp. 255-264, AISC, Vol. 316, 2015.

[2] Tang Jiali, Ren Gexue, *Modeling and Simulation of a Flexible Inverted Pendulum System*, Tsinghua Science and Technology, ISSN: 1007-0214, pp. 22-26, Vol. 14, Nr. S2, 2009.

[3] Tu Xu, Cuifang Zhang, *Multi-level Linear Flexible Inverted Pendulum Modeling*, Applied Mechanics and Materials, ISSN: 1662-7482, Vol. 518, pp. 290-296, 2014.

[4] Ashwani Kharola, Pravin Patil, *Fuzzy Hybrid Control of Flexible Inverted Pendulum (FIP) System using Soft-computing Techniques*, Pertanika Journal of Science & Technology, 25(4): 1189-1202, 20017.

[5] Minh Hoang Nguyen, Van Thuyen Ngo, Minh Tam Nguyen, Thi Thanh Hoang Le, Van Dong Hai Nguyen, *Designing Linear Feedback Controller for Elastic Inverted Pendulum with Tip Mass*, Journal of Robotica&Management, Vol. 21, Nr. 2, 2016.

[6] Sanket K. Gorade, Shailaja R. Kurode, *Mathematical Modeling of Flexible Inverted Pednulum on Cart with Tip Mass*, 27th Chinese Control and decision Conference, pp. 5584-5589, IEEE, 2015.

[7] S. van Mourika, H. Zwarta and K.J. Keesman, *Modelling and controller design for distributed parameter systems via residence time distribution*, International Journal of Control, Vol. 82, No. 8, pp. 1404–1413, 2009.

[8] Brian D. O. Anderson, John B. Moore, *Optimal Control: Linear Quadratic Methods*, (Dover Books on Engineering), 2007.

[9] Hong, Jie-Ren, *Balance Control of a Car-Pole Inverted Pendulum System*, Master Thesis, National Chengkung University, Taiwan, 2002.

Corresponding author:
Tran Ngoc Son
Ho Chi Minh City University of Technology and Education
Email: 1781106@student.hcmute.edu.vn